AD-753 411

FATIGUE BEHAVIOR OF THIN SOLID FILMS INDUCED BY A MOVING SURFACE LOAD

Richard A. Mollicone

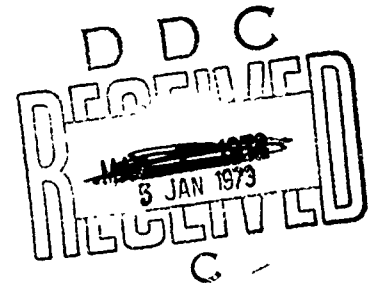Rensselaer Polytechnic Institute

AFML-TR-71-171

AD753411

FATIGUE BEHAVIOR OF THIN SOLID FILMS INDUCED BY A MOVING SURFACE LOAD

RICHARD A. MOLLICONE, MAJOR, USAF

TECHNICAL REPORT AFML-TR-71-171

FEBRUARY 1972

D D C
RECEIVED
5 JAN 1973
C

Approved for public release; distribution unlimited.

AIR FORCE MATERIALS LABORATORY
AIR FORCE SYSTEMS COMMAND
WRIGHT-PATTERSON AIR FORCE BASE, OHIO

NOTICE

When Government drawings, specifications, or other data are used for any purpose other than in connection with a definitely related Government procurement operation, the United States Government thereby incurs no responsibility nor any obligation whatsoever; and the fact that the government may have formulated, furnished, or in any way supplied the said drawings, specifications, or other data, is not to be regarded by implication or otherwise as in any manner licensing the holder or any other person or corporation, or conveying any rights or permission to manufacture, use, or sell any patented invention that may in any way be related thereto.

Copies of this report should not be returned unless return is required by security considerations, contractual obligations, or notice on a specific document.

AIR FORCE· 30-3-72/400

DOCUMENT CONTROL DATA - R & D

(Security classification of title, body of abstract and indexing annotation must be entered when the overall report is classified)

1. ORIGINATING ACTIVITY (Corporate author)	2a. REPORT SECURITY CLASSIFICATION
Air Force Materials Laboratory	UNCLASSIFIED
Wright-Patterson Air Force Base, Ohio 45433	2b. GROUP NA

3. REPORT TITLE

FATIGUE BEHAVIOR OF THIN SOLID FILMS INDUCED BY A MOVING SURFACE LOAD

4. DESCRIPTIVE NOTES *(Type of report and inclusive dates)*
Final - January 1965 to December 1966

5. AUTHOR(S) *(First name, middle initial, last name)*

Mollicone, R A.

6. REPORT DATE	7a. TOTAL NO. OF PAGES	7b. NO. OF REFS
February 1972	59	16

8a. CONTRACT OR GRANT NO	9a. ORIGINATOR'S REPORT NUMBER(S)
b. PROJECT NO 7342	AFML-TR-71-171
c. Task No. 734204	9b. OTHER REPORT NO(S) *(Any other numbers that may be assigned this report)*
d	

10. DISTRIBUTION STATEMENT

Approved for public release; distribution unlimited.

11. SUPPLEMENTARY NOTES	12. SPONSORING MILITARY ACTIVITY
	Air Force Materials Laboratory (LNL)
	Air Force Systems Command
	Wright-Patterson Air Force Base, Ohio

13. ABSTRACT

The purpose of this experimental study is to determine if a fatigue type failure and an endurance limit can be observed when a thin surface film is subjected to a normal load moving at a constant speed. Results of other research in related fields has indicated that particles of a surface coating become separated from the substrate prior to catastrophic failure of the coating when subjected to a moving load.

This mechanism of failure led Y. C. Hsu and F. F. Ling to accomplish an analysis of shear stresses in a thin film bonded to a base material. Their results related the shear stress at the interface to the speed of the load and material constants and indicated stress reversals that could be responsible for a fatigue type failure.

A test device was designed to subject coated specimens to moving normal loads of specific values. Various types of films were chosen with indium providing the basis for this study. Separation of particles from the substrate and from the coating itself were noted in all cases where failure occurred. Times to failure were analyzed statistically and plotted.

Experimental results agree with conclusions of the theoretical analysis. The data plots for indium coatings appear to indicate a fatigue behavior following the standard format for this type failure. Although no results are obtained from the other coatings chosen, there is sufficient reason to believe that thin films do exhibit fatigue failure under the type of loading described.

14. KEY WORDS	LINK A		LINK B		LINK C	
	ROLE	WT	ROLE	WT	ROLE	WT
SOLID LUBRICANTS						
FATIGUE BEHAVIOR						
GRAPHITE						
MOLYDENUM DISULFIDE						

☆U S Government Printing Office. 1972 — 759-084/449

AFML-TR-71-171

FATIGUE BEHAVIOR OF THIN SOLID FILMS INDUCED BY A MOVING SURFACE LOAD

RICHARD A. MOLLICONE, MAJOR, USAF

Approved for public release; distribution unlimited.

ic

FOREWORD

This report was prepared by Richard A. Mollicone, Major, USAF, Associate Professor, Department of Engineering Mechanics, United States Air Force Academy.

The study was supported in part by the Air Force Materials Laboratory and the Office of Aerospace Research under contract AF33(615)-3378 with Rensselaer Polytechnic Institute.

This report covers research work conducted from January 1965 to December 1966. The manuscript was released for publication by the author in February 1971.

This technical report has been reviewed and is approved.

R. L. ADAMCZAK, Chief
Fluid and Lubricant Materials Branch
Nonmetallic Materials Division
Air Force Materials Laboratory

ABSTRACT

The purpose of this experimental study is to determine if a fatigue type failure and an endurance limit can be observed when a thin surface film is subjected to a normal load moving at a constant speed. Results of other research in related fields has indicated that particles of a surface coating become separated from the substrate prior to catastrophic failure of the coating when subjected to a moving load.

This mechanism of failure led Y. C. Hsu and F. F. Ling to accomplish an analysis of shear stresses in a thin film bonded to a base material. Their results related the shear stress at the interface to the speed of the load and material constants and indicated stress reversals that could be responsible for a fatigue type failure.

A test device was designed to subject coated specimens to moving normal loads of specific values. Various types of films were chosen with indium providing the basis for this study. Separation of particles from the substrate and from the coating itself were noted in all cases where failure occurred. Times to failure were analyzed statistically and plotted.

Experimental results agree with conclusions of the theoretical analysis. The data plots for indium coatings appear to indicate a fatigue behavior following the standard format for this type failure. Although no results are obtained from the other coatings chosen, there is sufficient reason to believe that thin films do exhibit fatigue failure under the type of loading described.

TABLE OF CONTENTS

Preceding page blank

ILLUSTRATIONS

AFML-TR-71-171

TABLES

SECTION I

INTRODUCTION

1. HISTORICAL REVIEW

A solid lubricant can be defined as a material that provides lubrication to moving surfaces under dry conditions. This is accomplished by providing a thin film to separate the moving surfaces. In order to protect the surfaces and reduce friction, materials must be chosen with two important properties in mind. The material must have the ability to form a thin adherent film on the surface of a substrate material and the film material must be of low shear strength. Lamellar structured materials such as graphite and molybdenum disulfide have these properties in varying degrees and have been used for many years as solid lubricants. The need for lubrication under extreme environmental conditions na provided impetus for the study and use of many other solids as lubricants. Two distinguishing terms have been used by Merrill and Benzing (Reference 13) to categorize solid lubricants; solid-film lubricants and dry-film lubricants. Solid-film lubricants designate materials bonded to a bearing surface with some type of adhesive and dry-film lubricants refer to materials which react chemically with the substrate or are plated on the substrate.

Since solid lubricants have finite wear lives, the use of a system must be planned within the expected life of the lubricant. There have been many occurrences of early failures in systems utilizing solid lubricants, where the film has "flaked" and been removed from the system

allowing the moving parts to seize. Experimental work on surface temper-
atures of sliding systems (References 12, 15) including systems with
dry-film coatings, has suggested that catastrophic breakdown or failure
of the coatings was preceded by pieces of the film becoming separated
from the substrate due to repeated loading. Earlier experiments with
graphite subjected to repeated transversals of a point load
(Reference 11) have shown that flaking of the surface layers is related
to the stress applied and the number of cycles of application. Further
investigation by Lancaster and Clark (Reference 1) has indicated that
the failures of carbons are started by relative movement and fracture
beneath the surface layer. This is most likely due to the fact that
the point of maximum shear stress, and therefore the point with the
greatest tendency toward plastic deformation, is located just below
the surface (Reference 2).

Based on these observations Hsu and Ling have postulated
(Reference 7) that the shear strength of a film-substrate interface is
a function of cyclic stress application. Specifically, the higher the
applied stress the lesser the number of cycles that are required to
reach this shear strength or fatigue shear strength. Whenever the
fatigue shear strength of the film-substrate interface is reached, the
film becomes separated from the substrate at A as shown schematically
in Figure 1. Eventually the continued cycling will cause the film to
fail at B (Figure 1), allowing the piece of film to be removed from the
system as debris.
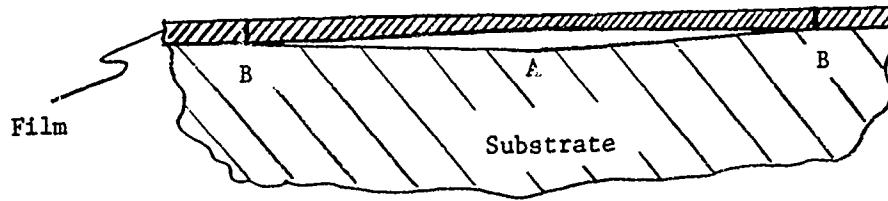
Figure 1. Schematic of Film-Substrate Separation

The mechanism of failure led Hsu and Ling to accomplish an analysis (Reference 7) of shear stresses in a thin film bonded to, or adhered to, a base material. These stresses were to be applied by a surface load moving at a constant velocity.

The maximum shear stress at the interface, given in terms of material parameters (the Lamé constants and density), was related to speed. Three regimes of speed (subsonic, transonic, and supersonic as defined by a local Mach number) were analyzed and their effects on the fatigue life of several layer-substrate combinations were discussed. Results indicated that failure could be of the fatigue type. Fatigue failure would occur more readily in the transonic than in the subsonic regime due to the increased number of shear stress reversals in the transonic regime.

Fatigue failure is the end result of the progressively destructive effect of repeated load cycles. Localized permanent changes take place in the submicroscopic and microscopic structure of a material. These changes, particularly in the early stages of fatigue damage, affect the progress of fatigue. Striations or highly localized slip bands form in the material and further reversed loading widens and intensifies these bands.

Strain-hardening may predetermine the subsequent formation and propagation of fatigue cracks, since the fatigue process apparently sets in when strain hardening has been essentially completed (Reference 4). Just as slip takes place in the striations of an annealed material, it also takes place within the sub-boundaries created by coldworking the material.

Continued cycling intensifies heat production on slip planes and the bands widen by further slip within the striations. Localized slip now causes microcracks to form, especially where the striations meet grain boundaries. These are areas of severe stress in a crystal and tend to block dislocation movement and prevent growth of striations. From this point on, microcracks propagate until failure occurs on the macro-scale. The interface of a coating and steel substrate is an area of extremely severe stresses, and as such should develop microcracks at an early stage. Freudenthal (Reference 4) makes a simple assumption that the number of cycles producing fatigue failure (N - No) is an inverse function of the density of striation areas per unit volume (1/s), where s is the mean spacing of striations:

$$(N - No) = K_1 (1/s)^{-q}.$$

There is a linear relationship between the density of slip bands (η) and the amount of strain hardening of an annealed material. The increase in applied shear stress (τ) over the elastic limit stress (τ_o) is proportioned to n:

$$(\tau - \tau_o) = k \cdot \eta.$$

Since $\eta \approx 1/s$, then $1/s \approx \dfrac{(S - S_o)}{k}$ where S and S_o represent general stress terms. Substitution in the basic assumption above gives:

$$(N - N_o) = K (S - S_o)^{-q}.$$

This is the same form that has been used to express the relationship between stress and cycles in fatigue testing. One can show that the applied stress (S), or σ_{12} as Hsu and Ling (Reference 7) term it, has a fixed relationship to the applied load (P). This is shown in Equation 60 of Appendix I. When the fatigue experiment is designed, then

$$(N - N_o) = K^1 (P - P_o)^{-q},$$

may be used as the form of the fatigue curve.

2. STATEMENT OF THE PROBLEM

The present experimental study has been motivated by the indications in the many scholarly works previously cited, but primarily by the conclusions of Hsu and Ling. It is the purpose of this study to determine if a fatigue type failure and an endurance limit can be observed when a thin surface film is subjected to a normal load moving at a constant speed. The speed of the load and the effect on surface film failure will be related in the sense of the local Mach number (M), as defined by Hsu and Ling. M is the ratio of the load velocity (V) to the shear wave velocity (C_2).

It was decided to investigate the failure characteristics of several layers of films on substrates of steel. Load speed was chosen so as to remain in the subsonic regime in the layer material and the steel substrate. This was done due to considerations of apparatus and specimen design and material availability, as well as in the interests

5

of limiting the scope of the experiment. The experiment was designed to

obtain statistical distributions of specimen failures at various load

levels. Recommendations of the American Society for Testing and Mate-

rials, Committee on Fatigue (E-9), were utilized in so far as possible

and the fatigue life curves were plotted with the aid of ASTM-STP91A

(Reference 5) and various distribution plots (Reference 10).

SECTION II

EXPERIMENTAL STUDY

1. EQUIPMENT DESCRIPTION

a. Specimen Design

The decision was made to utilize flat specimens rather than circular ones used in prior studies. This was based on the greater cost involved in coating circular specimens and the large number of specimens needed for the planned statistical analysis. In order to relate the present experimental results to prior observations of similar experiments, the linear speed of the moving normal load was to be made equivalent to the constant 1200 RPM and one inch radius used by Ling and Simkins. Since a reciprocating motion would be required and a constant speed desired a distance of two-thirds of the stroke length (ℓ_c) was used for the constant speed part of the motion. This is to allow for a sufficient length of specimen where the load is applied at a constant velocity. Based on circular specimens of radius one inch rotating at 1200 RPM, the following relationship between cam speed (n_c) and stroke length (ℓ_c) was calculated,

$$\ell_c = 2800/n_c.$$

The length of the stroke was chosen as one and one half inches and a cam speed of 1725 RPM; the considerations being available motors and a realistic length of observable specimen. For clearance purposes, the specimens were machined two inches in length.

With the value of stroke length chosen as one and one half inches, the portion of the specimen designated to be loaded at a constant speed

7

is one inch. This allows one quarter inch at each end of the stroke for the load to change its direction of motion. The calculations in Appendix II indicate that there will be no abrupt changes in stress at the interface due to the change in direction of the applied load. A width of one quarter of an inch was chosen to provide a uniform load application across the specimen without requiring too large a surface to be coated. The third dimension was chosen as one quarter of an inch to permit one quarter inch square drill rod to be used to manufacture the specimens. (Specimen dimensions are 1/4" x 1/4" x 2").

The coatings to be tested were chosen from those available at the time of the experiment and in as far as possible to give a variety of film types. Indium, gold, chromina, and alumina were to be used in the experimental analysis. The indium and gold were electroplated by commercial firms to a thickness of 0.0005 inches. This value was indicated by the literature as one most commonly specified in the interests of wear life and economy. DiSapio (Reference 3) to cite one of many, refers to 0.0005 inches as a desirable film thickness. The chromia and alumina specimens were flame plated by Linde Company of Union Carbide to a thickness of 0.005 inches since this was the thinest coating available within the limits of Linde flame spraying technology.

b. Apparatus Design

The size of the motor necessary to provide the desired reciprocating motion and speed was based on a maximum applied normal load and a slider tip width sufficient to give at least one stress reversal over the width of the tip. Hsu and Ling have indicated that the maximum

shear stress at the interface of the film and substrate occurs at a distance from the center of the applied load equal to ten times the film thickness (Reference 7). Since the local Mach number for this case is subsonic and approximately zero ($M \cong V/C_2$) a value of slider tip width (l_s) no less than 0.02 inches is indicated.

The width of the slider tip was chosen as 0.025 inches and was cut from a cylinder of radius 0.392 inches in order to reduce the possibility of ploughing.
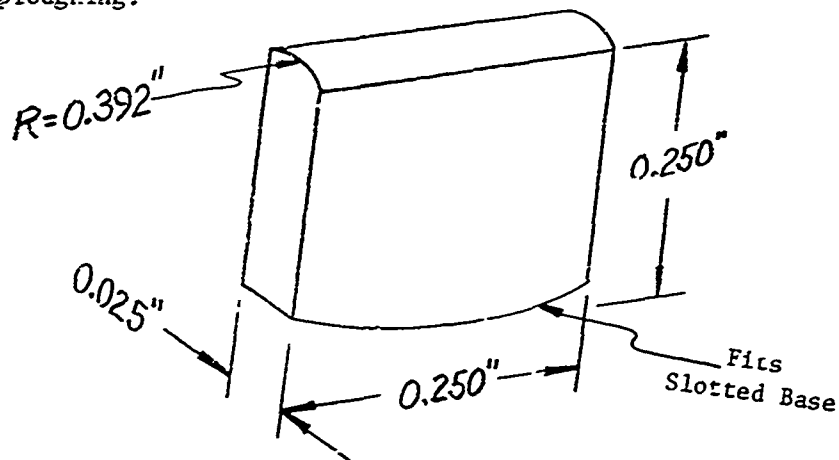
Figure 2. Sketch of Slider Tip

The relationship for Hertzian contact stresses between a cylinder and a plane is (Reference 6):

$$\sigma_n = 0.591 \sqrt{\frac{PE}{W_s R}} \; ;$$

where R is the radius, W_s is the length of the load, P is the load and E is Young's Modulus. With R = 0.392, E = 1.57 X 10^6 psi, W_s = 0.25 inches and σ_n = 15,000 psi, P_{max} = 40 lb. The initial coefficient of friction (μ) was chosen arbitrarily as 0.10 maximum and a 1725 RPM motor with 1/3 hp was used.

9

The Ferguson Machine Company of St. Louis, Missouri designed and built a housed barrel cam unit to meet the required specifications of speed and stroke length. One quarter revolution of the cam (matched to the 1725 RPM of the motor) was allocated to decelerate, stop, and accelerate the applied load to the constant lineal speed. One quarter revolution provides the constant speed of approximately 9.5 fps or 115 ips. The cam assembly is enclosed in an oil filled housing to provide lubrication and dampen vibrations. Venting of the sealed housing to the atmosphere was necessary to reduce frothing of the oil.

A flexible coupling joins the motor shaft to the cam shaft to ensure against misalignment and a cam rider provides the take off for the cam throw. Both the cam shaft and the cam rider shaft are mounted in brass bearings with O-ring seals.

The test apparatus itself consists of three main parts; the body, the specimen mounts, and the slider assembly (Figure 3). To ensure precise positioning of the moving load with respect to the specimens, the body was machined from one piece of stock. Specimen mounts are positioned by mount supports with shoulders to align the mounts and fix the distance between mounts (and thus specimens) to within 0.001 inch. The mount supports were designed to allow no vertical deflection of the specimen mounts (less than ten microinches) as well as to act as mechanical transducers for forces in the horizontal plane. Specimens were held in the slot in the mounts (Figure 3.B) by a positioning block which also allowed for minor corrections to the initial distance between specimens by means of shims. The slider assembly (Figure 4) provides the desired constant velocity to the applied load
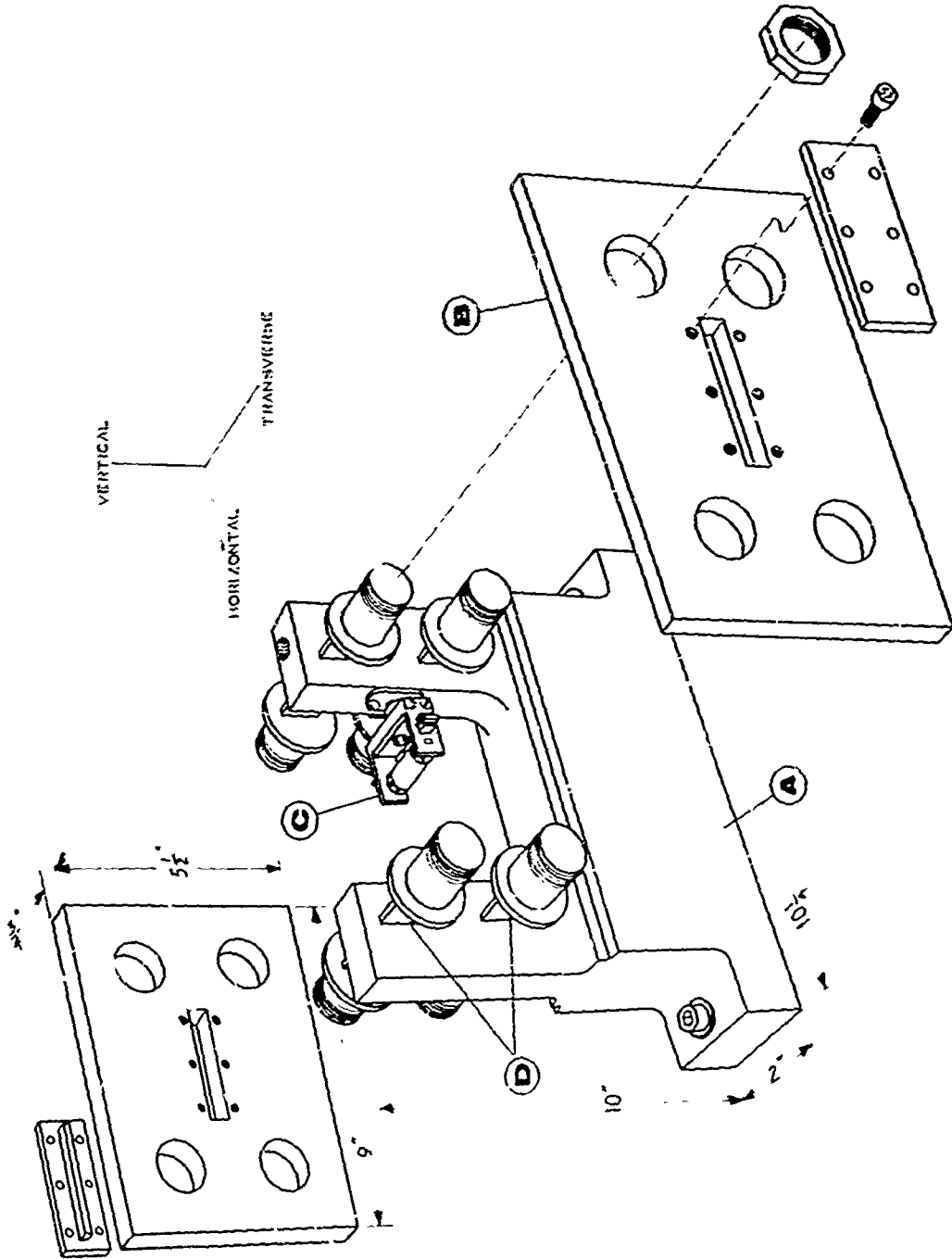
10

VERTICAL

TRANSVERSE

HORIZONTAL

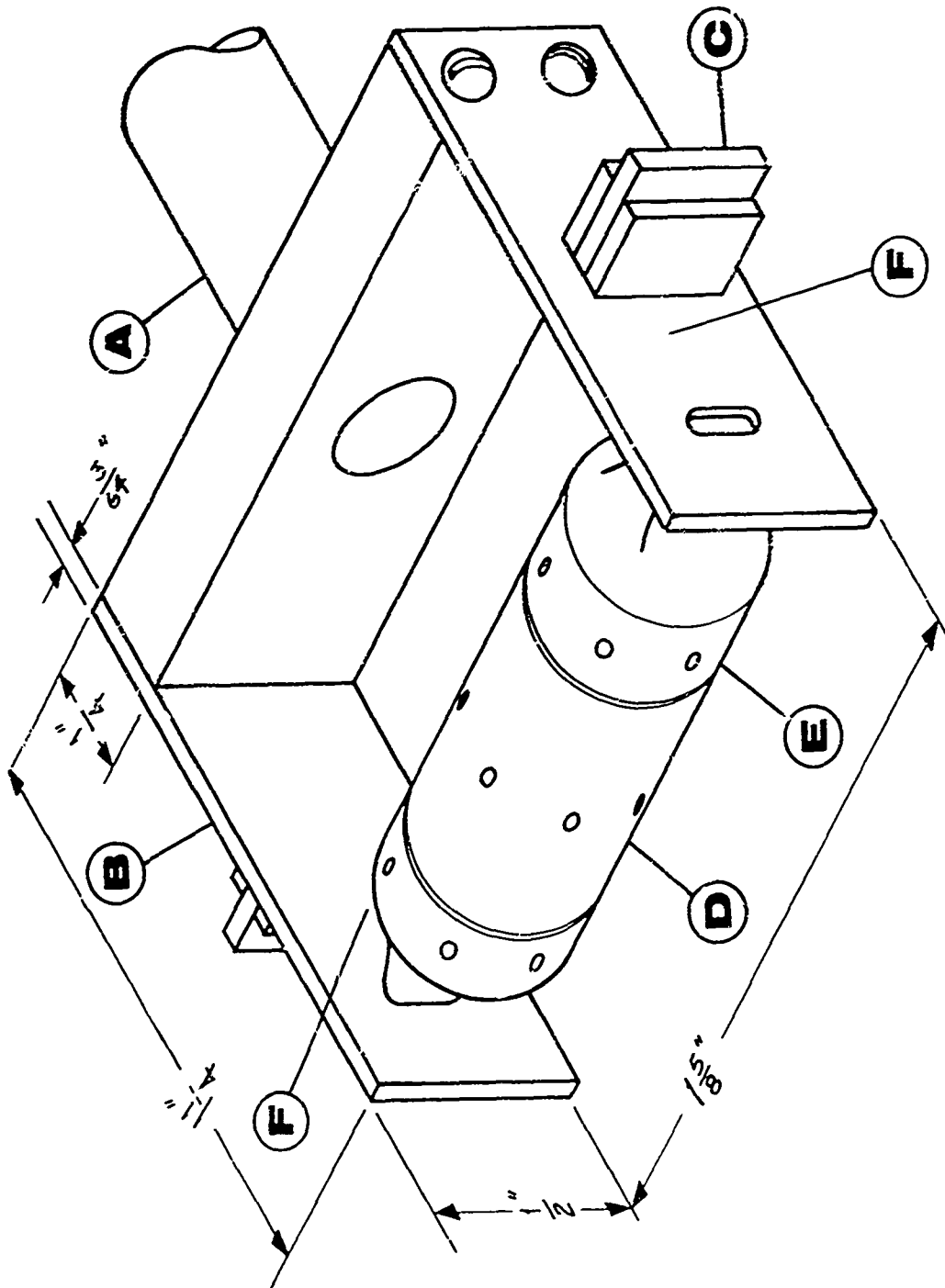Figure 3. Exploded View of Test Apparatus

11

Figure 4. Detail of Slider Assembly

by means of a hollow slider rod which is attached to the cam rider with a sleeve and is threaded into the slider base. Two thin arms mounted on the base transmit a force to the slider tips and also act as indicators for the load applied to the specimens. A collar with 10-48 left- and right-hand threads provides the force to slider arms, when it is rotated, and two lock nuts fix the position of the collar in place. The collar and lock nuts are rotated with minature spanner type wrenches. Due to the high velocities involved the slider rod is continuously lubricated with light oil dripping through a drilled passage in the body of the apparatus. Felt inserts in the bushings insure that the rod is evenly lubricated.

The slider tips are machined from Vascojet 1000, a high strength vanadium alloy steel. They are held in a slot with a circular arc base in the tip mount. This keeps the tips aligned properly with the specimens.

2. INSTRUMENTATION

a. Recording Device

A Sanborn Twin-Viso Recorder (Model 60-1300B) was used to monitor and record the outputs of the two strain gage circuits. Each gage circuit signal was amplified by a Sanborn Strain Gage Amplifier (Model 64-500B) connected directly to the recorder. This model recorder provided sufficient channels for the experiment and a wide range of signal presentation on a moving paper. Paper speed could be varied up to 100 mm per second to give a distinct reproduction of all signals. This was accomplished by a recording arm whose amplitude was a response
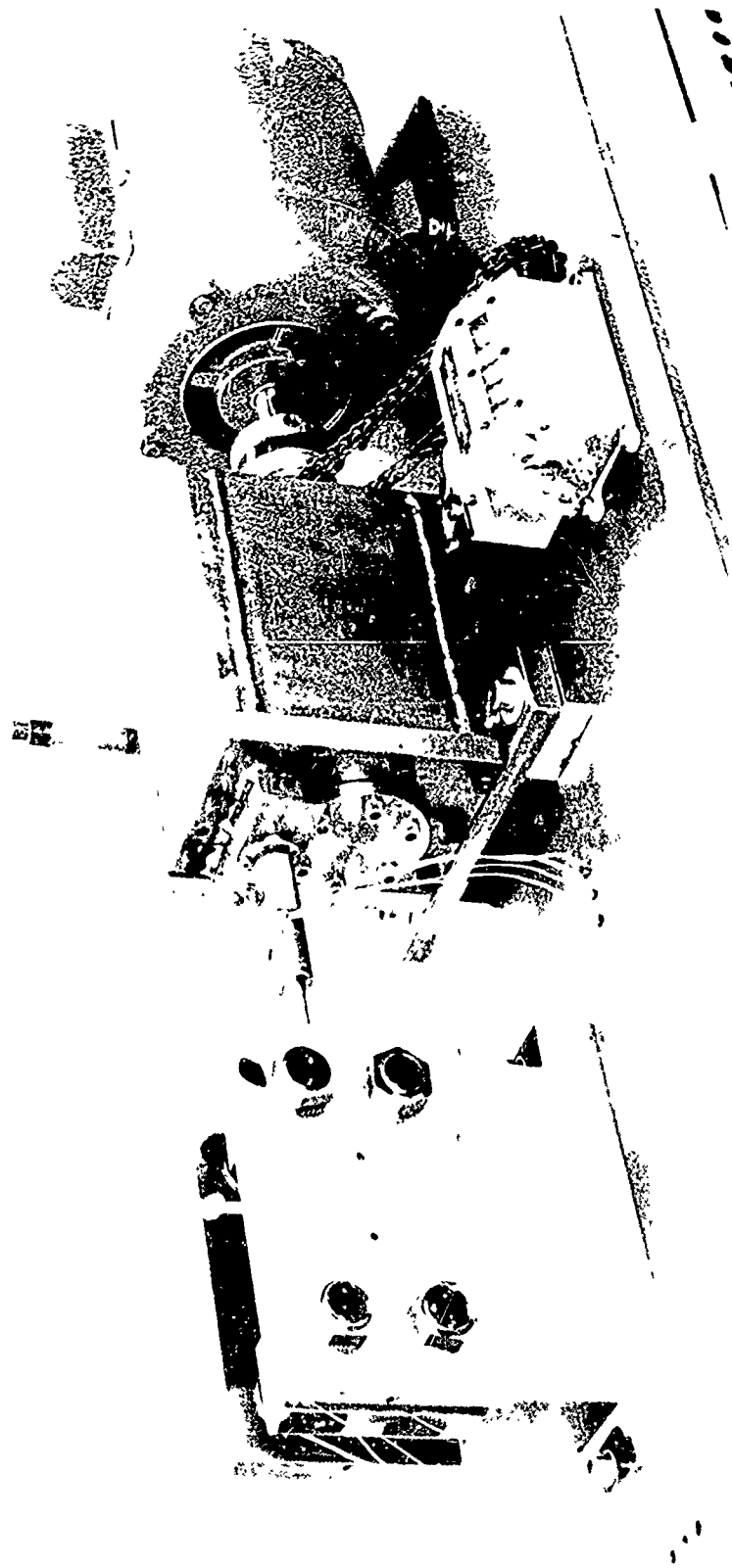
13

Figure 5. Assembled Test Device
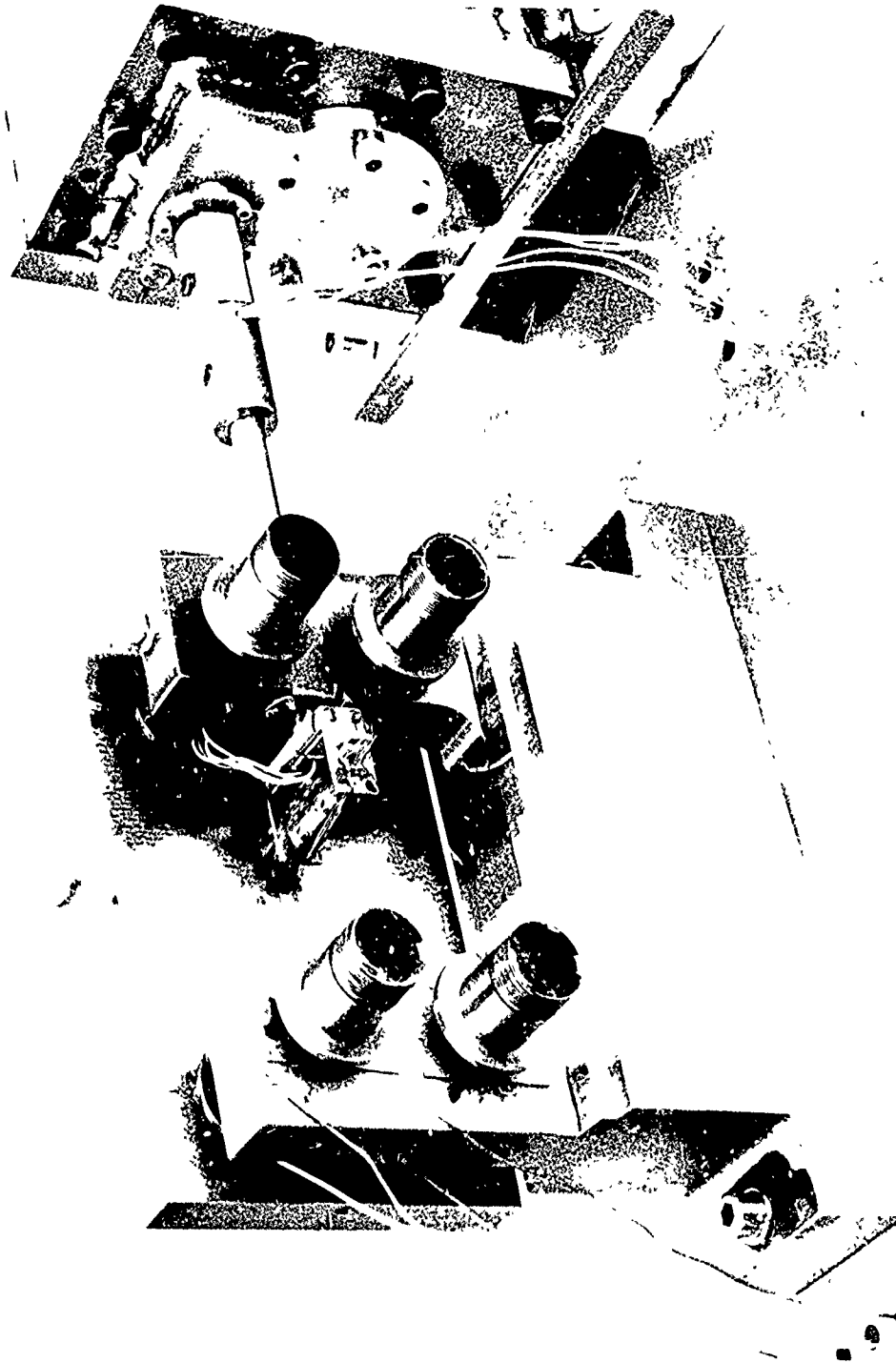
Figure 6. Partially Disassembled Test Device

to these input signals. Instructions for the physical setup and operation of the recorder and amplifiers were taken from Sanborn Company manuals (References 8, 9).

b. Strain Gage Circuits

All strain gages used in the circuitry are SR-4 type, 0.06 inches constantan foil gages with a paper base (FAP-06-12-S-9).

Two gages were centered on each slider arm one quarter of an inch from the point where the collar applies the force to each arm (Figure 4. F). This takes advantage of the largest induced bending moment without interference from the slider tip mount. The gages were connected in such a manner that indicated strains would be additive and give the greatest unbalance to the bridge circuit. All of the leads were insulated with varnish and soldered to wires running through the hollow slider rod to terminals on the connecting sleeve. From this point the circuit was completed to the Sanborn amplifier for the applied load.

Monitoring of the friction forces was accomplished in a similar manner on the other channel of the Sanborn recorder. Two strain gages were centered on either side of each mount support (a total of eight gages) close to the apparatus body (Figure 3. D) in order to measure the strains caused by the maximum bending moment. The supports utilized were those at the end of the body without the slider rod bushing.

c. Calibration of Applied Load Circuit

Each slider arm w   calibrated individually in order to match their ber ng characteristics. Preliminary calculations indicated that the

load applied to the specimens by the slider tips would be approximately

three times the force applied to the slider arms by the loading collar.

A slider arm was mounted on a jig to simulate actual conditions

(Figure 7) and loaded in one pound increments (F) up to 20 pounds. This

gave values of P (load applied to the specimen) well over the maximum

planned value of 40 pounds. Strain readings (ϵ) were recorded as a
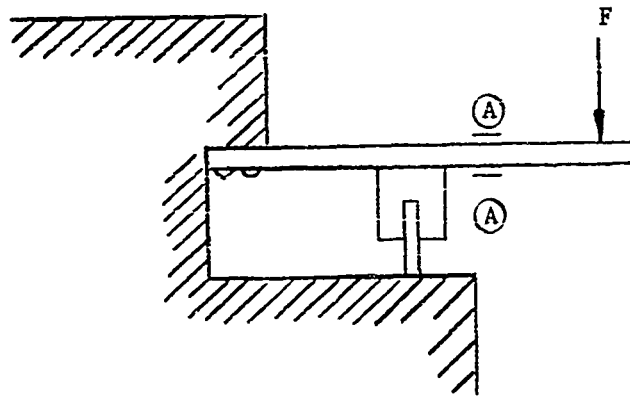
function of the force (F) for each arm.

Figure 7. Slider Arm Calibration Jig (F vs ϵ)
(A.) Strain Gages

Slider tips were given a light coating of Molycote to prevent adhesion

between the tip and jig interface. Now the arms were mounted on another

jig (Figure 8) and loaded with the force (F).
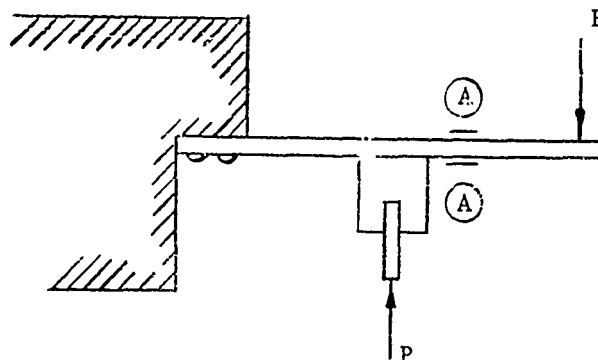
Figure 8. Slider Arm Calibration Jig, (P vs ϵ)
(A.) Strain Gages

The force (P) was applied until the strain readings corresponding to each value of F were indicated. This force, P, is the load to be applied to the specimens and will be indicated by a strain reading on the recording device. Table I compiles the averaged calibration data for the assembled slider. The relationship between the strain (in microinches per inch) and the load to be applied (in pounds) is;

$$\epsilon = 8.33 \ P.$$

Once the relationship between the applied load, P and a measured strain, ϵ was known, the Sanborn recorder had to be calibrated in order to set, record, and monitor the applied load during each test run. Deflections for various applied loads were calculated (Reference 8) and are compiled in Table II.

d. Calibration of Friction Force Circuit

Before calibrating the friction force circuit, a check was made to see if dynamic calibration was necessary. Since the ratio of the excitation frequency to the systems natural frequency is very close to one a static calibration was performed.

In order to load both specimen mounts symmetrically in the horizontal plane, a loading jig was constructed so a force could be applied at one point. The mounts were loaded in one pound increments and a strain reading ϵ (in microinches per inch) was recorded for each force S (in pounds) up to 20 pounds. The data is compiled in Table III and when corrected to zero is expressed by the formula;

$$F = .09 \ \epsilon.$$

TABLE I

SLIDER ASSEMBLY LOADING CALIBRATION; = 8.33P

APPLIED LOAD P (lb)	INDICATED STRAIN ϵ (μ in/in)
2	16
5	41
10	83
12	100
14	116
15	125
20	166
24	200
25	208
26	217
30	250
35	292
38	317
40	334
42	350
45	375
50	416

TABLE II

SANBORN RECORDER CALIBRATION
APPLIED LOAD AS A FUNCTION OF SIGNAL DEFLECTION

APPLIED LOAD P (lb)	INDICATED STRAIN ε (μ in/in)	ATTENUATOR SETTING	DEFLECTION (cm)
2	16	1	1.60
5	41	5	0.82
10	83	5	1.65
12	100	5	2.00
14	116	10	1.16
15	125	10	1.25
20	166	10	1.66
24	200	20	1.00
25	208	20	1.04
26	217	20	1.09
30	250	20	1.25
35	292	20	1.46
38	317	20	1.59
40	334	20	1.67
42	350	20	1.75
45	375	50	0.75
50	416	50	0.83

TABLE III

CALIBRATION OF SPECIMEN MOUNT SUPPORTS

FORCE S (lb)	STRAIN ε (μ in/in)
0	0
2	12
3	21
4	31
5	44
6	54
7	68
8	79
9	93
10	106
11	121
12	132
13	142
14	152
15	164
16	177
17	191
18	201
19	210
20	220

Strains are calculated from deflections (in centimeters) of the recording arm by means of the following relationship (Reference 8);

$$\varepsilon = \left[\text{Deflection}\right]\left[\text{Attenuator Setting}\right]\left[\text{Basic Sensitivity}\right].$$

Using the value of 20 as the basic sensitivity of this circuit, Table IV compiles values of strain for various deflections and attenuator settings.

3. TEST PROCEDURES

For the purposes of this experiment, and to exclude the phenomenon of wear, failure of a specimen was defined as the time at which the first significant change in friction was observed. When the normal load P is applied, the slider arms are fixed in position. Any wear of the surface coating will be indicated by a gradual decrease in the friction force to a constant value. Trial runs showed this to be true. Conversely, any large and rapid decrease in the friction force would indicate the removal of particles of the coating from the system. Examination of the recorded data and the specimens for the trial runs indicated that there was a pileup of coating particles at either end of the specimens and sharp changes in the friction force for the trial loads used, although there was nothing to tie the two facts together. However, it was noted that there was a significant sharp rise in the plot of the applied load at the same time coordinate that was indicated for the change in the friction force. It was reasoned that this was due to the removal of coating particles from the system and subsequent jamming of these particles under the slider tip, thus giving a momentary sharp rise in the applied force, Γ. Therefore the indications on the

TABLE IV

CONVERSION FROM DEFLECTION TO STRAIN

Deflection (cm)	Attenuator Setting	ε (μ in/in)
0.50	1	10
1.00	1	20
1.50	-	30
2.00	1	40
2.50	1	50
1.00	2	40
1.50	2	60
2.00	2	80
0.80	5	80
0.90	5	90
1.00	5	100
1.10	5	110
1.20	5	120
1.30	5	130
1.40	5	140
1.50	5	150
1.60	5	160
1.70	5	170
1.80	5	180
1.90	5	190
2.00	5	200

friction force plot, as well as the applied load plot, were utilized to give a time to failure for each specimen. As an additional trial, specimens loaded with P less than five pounds showed a gradual decrease in the frictional force plot and no significant rise on the applied load plot.

On the basis of the trial runs and recommendations of the ASTM manual (Reference 5), experimental data was to be taken at the applied loads listed below with at least 15 specimens to be tested at each load level except for $P = 2$ lb where eight specimens were tested.

$$P = 35 \text{ lb}$$
$$P = 30 \text{ lb}$$
$$P = 25 \text{ lb}$$
$$P = 20 \text{ lb}$$
$$P = 14 \text{ lb}$$
$$P = 10 \text{ lb}$$
$$P = 5 \text{ lb}$$
$$P = 2 \text{ lb}$$

The value of $P = 14$ lb was chosen due to an initial mistaken setting on the recorder and intentionally carried through the experiment. An arbitrary value of $P = 2$ lb was chosen as one value below $P = 5$ lb. Trial run experience showed that no indications of failure by $t = 10$ seconds could be considered a run-out.

It should be noted that each pair of specimens provides only one data point. The specimens are tested in pairs in order to preclude any variation in the applied load P due to bowing of the slider arm.

SECTION III

EXPERIMENTAL DATA

1. DATA

The first series of specimens were indium plated with a coating thickness of 0.0005 inches. Sequencing of planned loads was done in a random manner until all load levels had sufficient data points. Then five to eight more runs were made at $P = 10$, 20, and 30 pounds. Table V presents the data by load level in an ordered tabulation. All six data points for $P = 2$ lb were run-outs.

Reduction of the data in Table V was accomplished according to the guidelines set down in the ASTM manual on fatigue (References 5, 10) and the fact that a normal distribution of log time to failure can be expected in the analysis of fatigue data (References 4, 14). Data for three curves was calculated and is tabulated in Table VI. Mean log t at each load was calculated for the standard fatigue curve; the 50% survival curve at 50% confidence level. The same thing was done for a 75% survival curve at 50% confidence level and a 90% survival curve at 95% confidence level. It should be noted that mean log t values for load levels near the fatigue limit, particularly where run-outs are involved, are better calculated by the Weibull distribution method (References 10, 16). Rectified values of time to failure $(t - t_o)$ plots as a straight line indicating a Weibull distribution. Data for $P = 5$ lb and $P = 10$ lb is listed in Tables VII and VIII and is plotted on Weibull distribution paper in Figures 9 and 10. When $F(t) \times 100 = 63.2\%$, $t = 0.19$ seconds for

25

TABLE V

ORDERING OF SPECIMENS BY LOAD LEVEL

ORDER No., q	a = 1 5 lb	a = 2 10 lb	a = 3 14 lb	a = 4 20 lb	a = 5 25 lb	a = 6 30 lb	a = 7 35 lb
	t_i	t_i	t_i	t_i	t_i	t_i	t_i
1	0.04	0.05	0.045	0.05	0.05	0.024	0.048
2	0.06	0.05	0.084	0.054	0.05	0.042	0.052
3	0.06	0.05	0.09	0.057	0.054	0.048	0.054
4	0.06	0.05	0.10	0.058	0.054	0.054	0.054
5	0.06	0.05	0.11	0.058	0.058	0.056	0.054
6	0.08	0.054	0.12	0.058	0.058	0.056	0.054
7	0.08	0.054	0.12	0.058	0.06	0.058	0.055
8	0.12	0.058	0.12	0.06	0.06	0.058	0.056
9	0.12	0.064	0.124	0.06	0.078	0.060	0.056
10	0.142	0.07	0.14	0.065	0.084	0.060	0.058
11	0.16	0.07	0.14	0.092	0.088	0.062	0.06
12	0.20	0.085	0.175	0.092	0.088	0.076	0.06
13	0.37	0.09	0.26	0.095	0.090	0.080	0.096
14	0.38	0.10	0.285	0.102	0.092	0.09	0.098
15	0.57	0.106		0.104	0.148	0.097	
16	1.00	0.116		0.108		0.098	
17	Run-out	0.122		0.124		0.10	
18		0.124		0.14		0.11	
19		0.138		0.155		0.11	
20		0.21		0.38		0.12	
21		0.26				0.14	
22						0.16	
23						0.75	

TABLE VI

VALUES OF $\hat{t}$ FROM RAW DATA IN TABLE V

LOAD P (lb)	$\hat{t}_a$*	$\hat{t}_b$**	$\hat{t}_c$***
2	Run-out	Run-out	Run-out
5	0.138	0.073	0.020
10	0.083	0.059	0.030
14	0.124	0.091	0.048
20	0.085	0.060	0.030
25	0.071	0.057	0.037
30	0.082	0.052	0.021
35	0.060	0.051	0.038

*$\hat{t}_a$: mean log t for 50% survival at 50% confidence level

**$\hat{t}_b$: mean log t for 75% survival at 50% confidence level

***$\hat{t}_c$: mean log t for 90% survival at 95% confidence level

TABLE VII

MEAN RANK ESTIMATES OF THE PERCENT SPECIMENS
FAILED. LOAD P = 5 LB FOR AN ORDERED SAMPLE
OF SIZE n = 17 (ONE RUN-OUT, n' = 16)

ORDER NUMBER	t(sec)	F(t) × 100	$\frac{(t - \hat{t}_o)}{\hat{t}_o} = 0.04$
1	0.040	5.56	0
2	0.060	11.11	0.020
3	0.060	16.67	0.020
4	0.060	22.22	0.020
5	0.060	27.78	0.020
6	0.080	33.33	0.040
7	0.080	38.89	0.040
8	0.120	44.44	0.080
9	0.120	50.00	0.080
10	0.142	55.56	0.102
11	0.160	61.11	0.120
12	0.200	66.67	0.160
13	0.370	72.22	0.330
14	0.380	77.78	0.340
15	0.570	83.33	0.530
16	1.000	88.89	0.960
17	Run-out		

TABLE VIII

MEAN RANK ESTIMATES OF THE PERCENT SPECIMENS
FAILED FOR AN ORDERED SAMPLE OF SIZE n = 20 LB. LOAD P = 10 LB

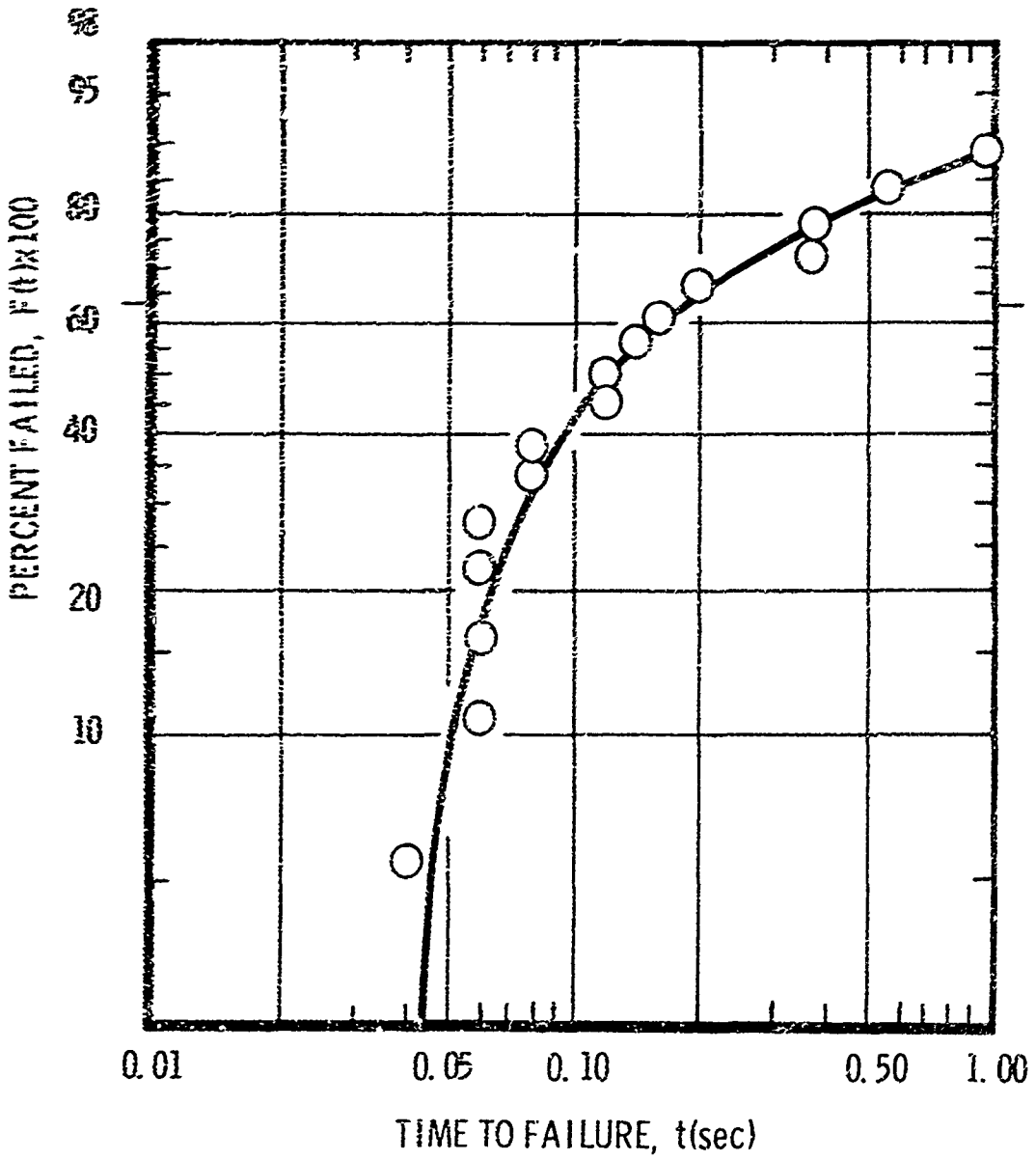| ORDER NUMBER	t (sec)	F(t) × 100	$\dfrac{(t - \hat{t}_o)}{\hat{t}_o = 0.044}$
1	0.050	4.76	0.006
2	0.050	9.52	0.006
3	0.050	14.29	0.006
4	0.050	19.05	0.006
5	0.054	23.81	0.010
6	0.054	28.57	0.010
7	0.058	33.33	0.014
8	0.064	38.10	0.020
9	0.070	42.86	0.026
10	0.070	47.62	0.026
11	0.085	52.38	0.041
12	0.090	57.14	0.046
13	0.100	61.90	0.056
14	0.106	66.67	0.062
15	0.116	71.43	0.072
16	0.122	76.19	0.078
17	0.124	80.95	0.080
18	0.138	85.71	0.094
19	0.210	90.48	0.166
20	0.260	95.24	0.216

Figure 9. Weibull Distribution for Time to
Failure, t, At Load, P = 5 lb
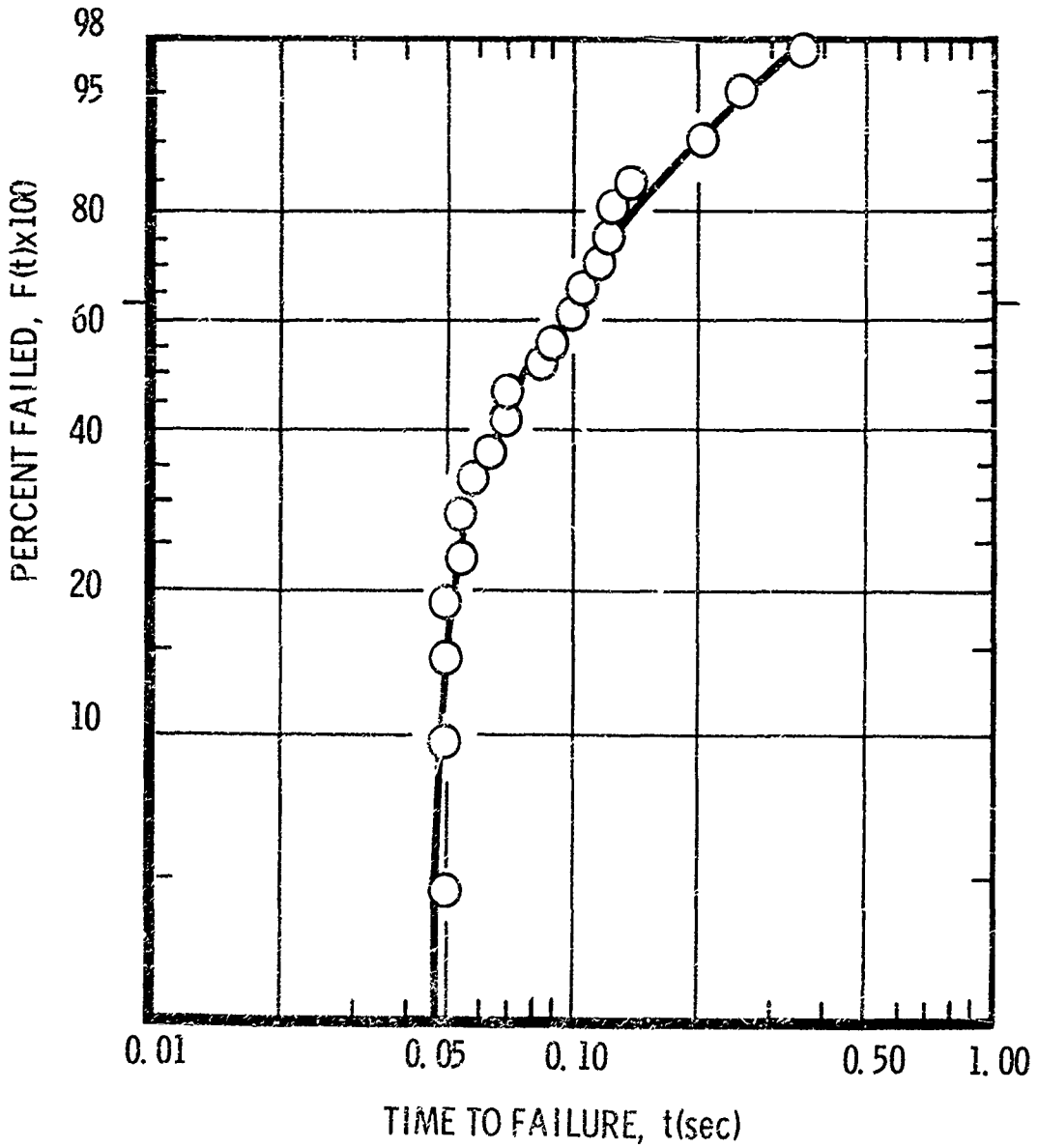
Figure 10. Weibull Distribution for Time to
Failure, t, At Load, P = 10 lb

P = 5 lb, and t = 0.095 seconds for P = 10 lb. These values and the values for mean log t for all other load levels are plotted as survival curves in Figures 11, 12, and 13.

No data was collected from any runs with the 20 chromia and 20 alumina coated specimens. The coatings on these flame plated specimens were powdered at all load levels used on the indium coated specimens. There were also no results from the gold plated specimens. The gold was ploughed off the surface with no indications of any time to failure.

Subsequent to completing all of the above test runs, two experimental low shear modulus silicone rubbers were obtained from the General Electric Company, Schenectady, New York, plant. Although General Electric directions for bonding these to steel surfaces were followed, all specimens peeled off when tested in the apparatus. As a result, no data was collected from these specimens.

2. DISCUSSION OF RESULTS

From the data plots for indium coatings in Figures 11, 12, and 13 it appears that failures of the film-substrate system do indicate fatigue behavior. An inspection of the specimens after each run showed evidence of particle separation within the coating as well as at the interface. This would seem to indicate that the maximum alternating shear stress had occurred within the film, although the stresses at the interface had still produced failure there.

Due to the number of run-outs at P = 2 lb, it would seem that there is also a fatigue limit, within the definition of failure used here, although this point might need further investigation.
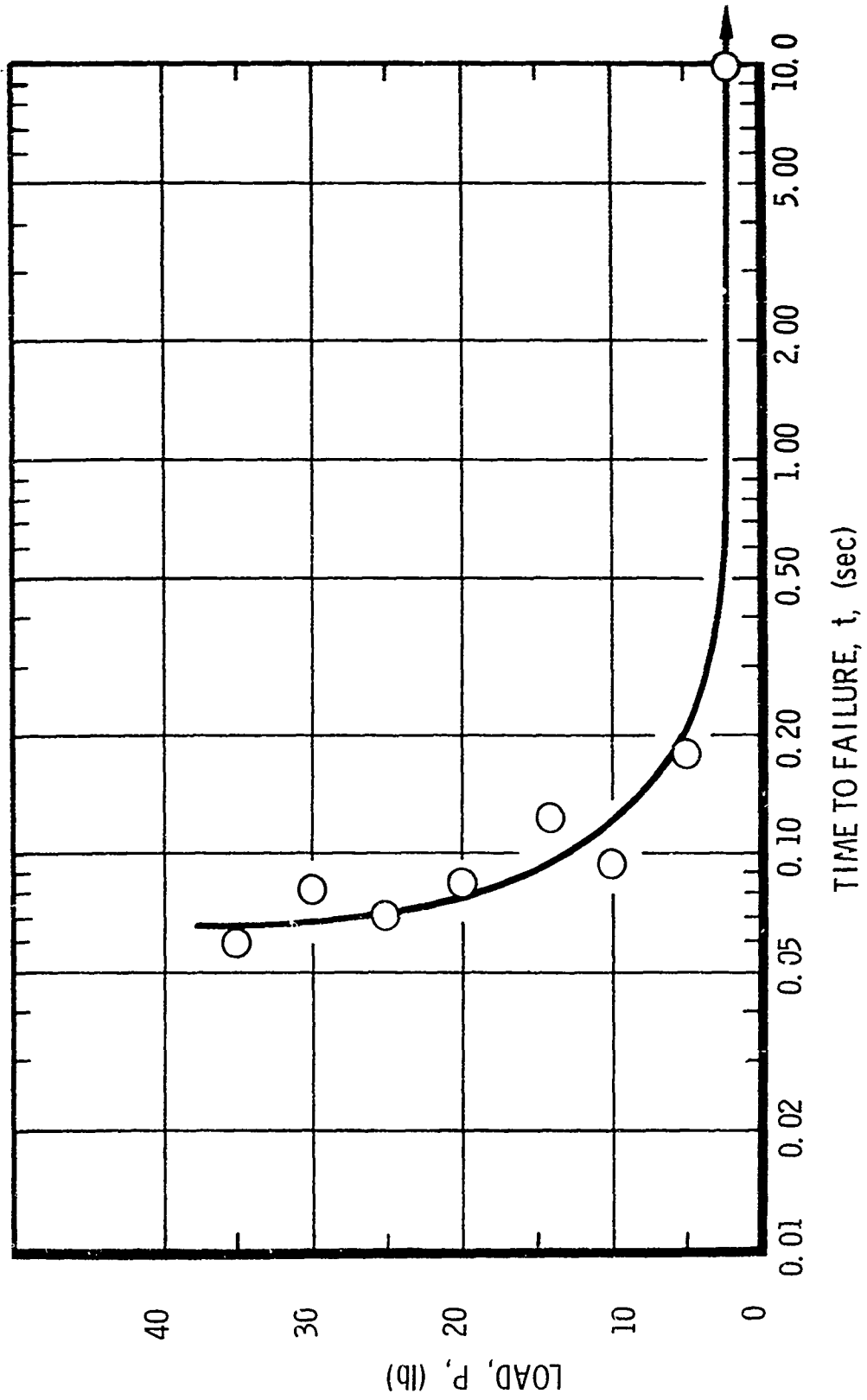
32

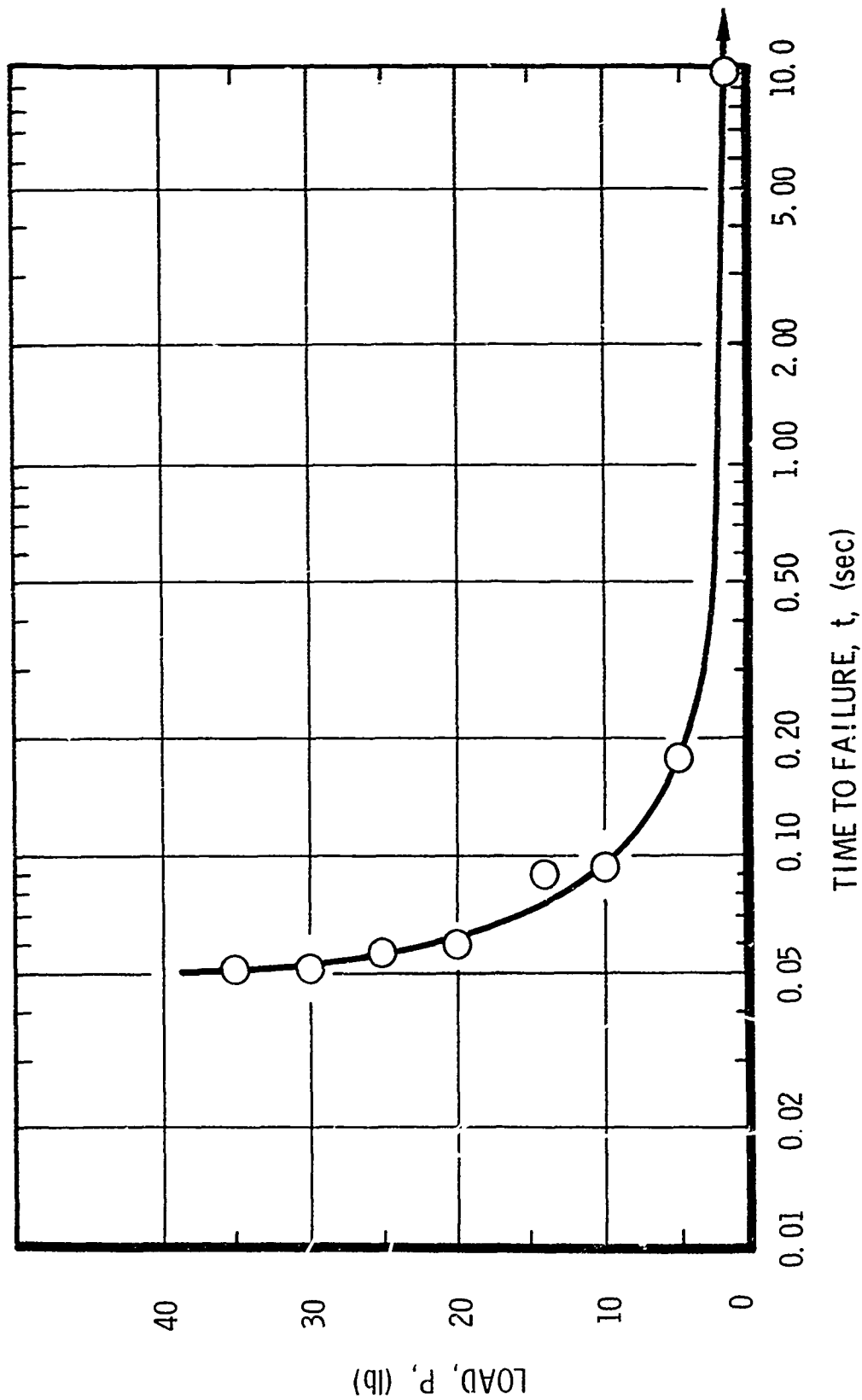Figure 11. 50% Survival Curve at 50% Confidence Level

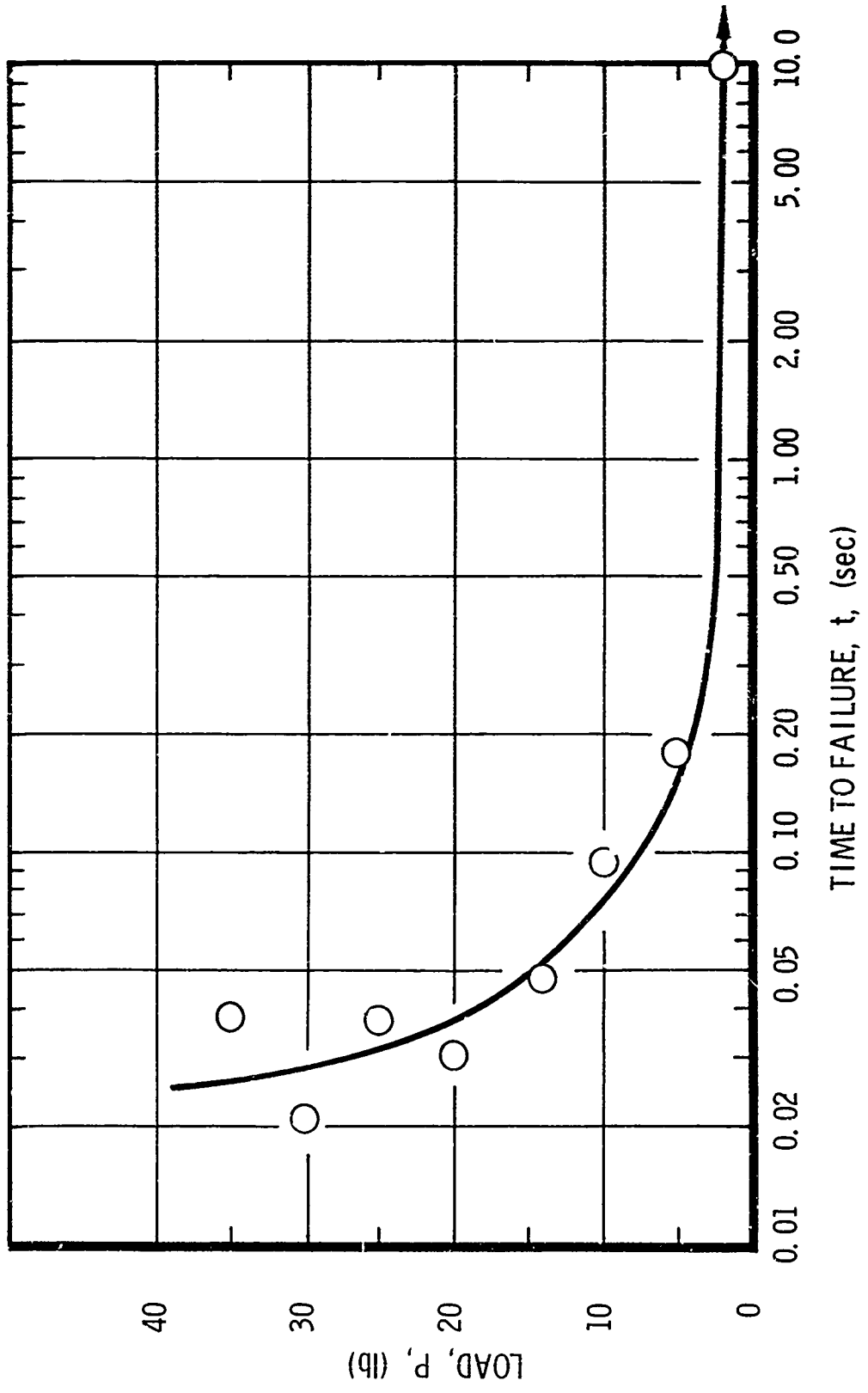Figure 12. 75% Survival Curve at 50% Confidence Level

Figure 13. 90% Survival Curve at 95% Confidence Level

The validity of this data lies not only in the indicated curve trends, but the manner in which the experiment was designed. Together they would give a high degree of confidence in the results.

It is unfortunate that the other materials tested did not yield any data. They would have provided corroborative data for materials with similar shear moduli. Apparently the quality of the gold plating was poor and could not be improved upon locally. Further tests on quality gold plating would be of great interest. There is no reason, according to the Linde Division of Union Carbide, for the chromia and alumina coatings to "powder". The only explanation the researcher can give is the possibility that the speed and type of loading involved combined to disintegrate the flame-plated particles so rapidly that failure could not be measured with the instrumentation used. It should also be noted that the quality of the plating with any of the coatings, will enter the picture as a parameter between types of coatings but not necessarily within a particular sampling.

SECTION IV

CONCLUSION

The need for using greater speeds in loading becomes obvious as the
search for coatings with lower shear moduli continues. With the present
setup, even if the silicone rubbers had yielded data, the analysis
would still have been in the subsonic regime. Modification of the
apparatus and the use of other materials are indicated for follow-on
experimentation. The possibility of a much higher speed of loading with
a roller-type applicator should be investigated.

SECTION V

REFERENCES

1. W. T. Clark and J. K. Lancaster, "Breakdown and Surface Fatigue of Carbons During Repeated Sliding," Wear, 6, 467-482 (1963).

2. R. M. Davies, "The Determination of Static and Dynamic Yield Stresses Using a Steel Ball," Royal Society of London, Proceeding, A197, 416-432 (1949).

3. Alfred Di Sapio, "Bonded-Lubricant Coatings," Machine Design, 35, 167-172 (1963).

4. Alfred M. Freudenthal, "Fatigue," Handbuch der Physik, VI, Springer-Verlag, Berlin, 591-611 (1958).

5. "A Guide for Fatigue Testing and the Statistical Analysis of Fatigue Data," ASTM STP No. 91-A (Second Edition) (1963).

6. Heinrich R. Hertz, Miscellaneous Papers (D. E. Jones), The MacMillan Company, New York, 163-178 (1896).

7. Y. C. Hsu and F. F. Ling, "Shear Stresses in a Layered Elastic System Under a Moving Load," Recent Advances in Engineering Science, Volume II, Gordon and Breach, New York, 323-351 (1965).

8. I. M. 60-1300-1, Sanborn Twin-Viso Recorder (Model 60-1300), Sanborn Company, Waltham, Massachusetts.

9. I. M. 140-1, Strain Gage Amplifier (Model 64-500B), Sanborn Company, Waltham, Massachusetts.

10. James R. King, Graphical Date Analysis with Probability Papers, Technical and Engineering Aids for Management Co., Lowell, Massachusetts (1969).

11. J. K. Lancaster, "Elastic Deformation and the Wear of Electrographite," Nature, 196, 368 (1962).

REFERENCES (CONT'D)

12. F. F. Ling and T. E. Simkins, "Measurement of Point-wise Juncture Condition of Temperature at the Interface of Two Bodies in Sliding Contact," Journal of Basic Engineering, Transactions of ASME, 85, 461-487 (1963).

13. C. F. Merrill and R. J. Benzing, "Solid Film Lubricants for Extreme Environments," Machine Design, 11, 208-210 (1963).

14. Cedric W. Richards, Engineering Materials Science, Wadsworth Publishing Co., Inc., San Francisco, 339-356 (1961).

15. T. E. Simkins and S. L. Pu, "Further Data on the Juncture Condition of Temperature at the Interface of Two Bodies in Sliding Contact," AD 422-460 (1963).

16. Waloddi Weibull, Fatigue Testing and the Analysis of Results, Pergamon Press, New York, pp 159-167, 198 (1961).

APPENDIX I

The following is excerpted from the chapter by Hsu and Ling in Reference 7. No attempt has been made to paraphrase or interpret their material.

Of interest here is the quasi-stationary behavior in plane-strain of an elastic system, consisting of a half-space with a layer on top, under a surface load moving at constant velocity. In particular, the maximum shear stress at the layer-base interface is sought.

The physical motivation of the problem is that of correlating the maximum shear stress to the fatigue life of the surface layer as a function of speed. Other parameters being the material properties and the nature of the load.

Mathematically, the problem is stated below. Given a semi-infinite solid with a surface layer of thickness H, the material properties are λ, μ, ρ, and λ^*, μ^*, ρ^*, respectively, where λ and μ are the Lamé constants and ρ is the density. The composite body is moving with a constant velocity V past a distributed load $p(x_1)$ for $-1 < x_1 < 1$, as shown in Figure 14. Considering the state of stress as being plane-strain, the quasi-stationary solution is found from the equation of motion with respect to the coordinates (x_1, x_2). Of particular interest is the shear stress at the interface of the layer and base material.

The equations of motion for the semi-infinite solid are

$$(\lambda + \mu)D_{,\alpha} + \mu U_{\alpha,\beta\beta} = \rho \ddot{U}_\alpha \quad (\alpha, \beta = 1, 2) \tag{1}$$

Preceding page blank

in which $D = U_{\beta,\beta}$, the subscript α after comma denotes partial differentiation with respect to x'_α ($\alpha = 1, 2$) and repeated indices denote
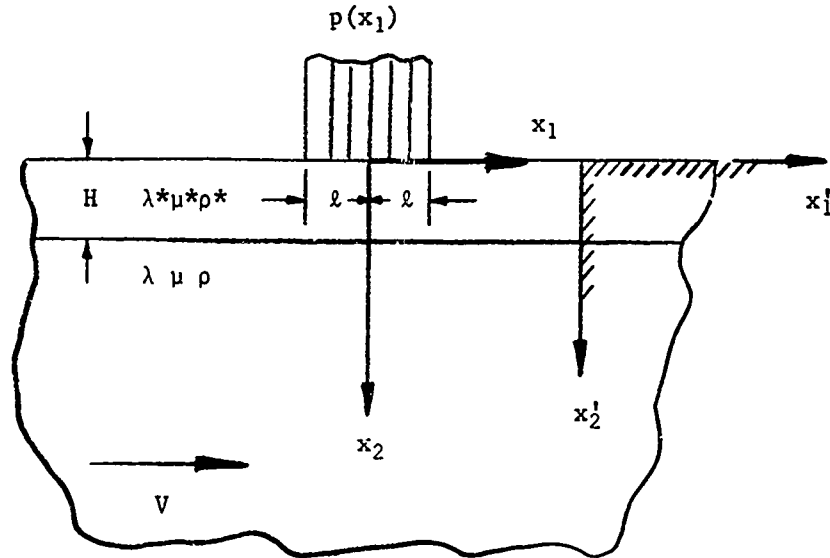

Figure 14. Composite Body Moving with a Constant Velocity
V Past a Distributed Load $p(x_1)$ for $-1 < x_1 < 1$

summation, U_α is the αth component of displacement and the super dots represent material time differentiation.

The stress-displacement relations are

$$\sigma_{\alpha\beta} = \lambda \, D \, \delta_{\alpha\beta} + \mu \, (U_{\alpha,\beta} + U_{\beta,\alpha}) \tag{2}$$

in which $\sigma_{\alpha\beta}$ is the _stress tensor_ and $\delta_{\alpha\beta}$ is the Kronecker _delta_.

Let (x'_1, x'_2) denote space coordinates fixed in the medium which occupies the semi-infinite solid $x'_2 > 0$, Figure 14. Consider the moving frame (x_1, x_2) fixed with respect to the load. For the problem at hand, it is convenient to use the Eulerian coordinates x_α where $x_1 = x'_1 + Vt$ and in which V is the constant velocity of motion of the composite material and t is the time. For the quasi-stationary state the material

derivative, for $\partial(\ )/\partial t = 0$ with respect to the moving frame $(x_1, x_2,$ is

$$\frac{D^2(\ )}{Dt^2} = V^2 \frac{\partial^2(\ )}{\partial x_1^2} \tag{3}$$

Equations 1 and 3 become

$$(\lambda + \mu) D,_\alpha + \mu U_{\alpha,\beta\beta} = \rho V^2 U_{\alpha,11}. \tag{4}$$

Similar equations with $\lambda*$ and $\mu*$ in lieu of λ and μ apply for the surface layer.

The boundary conditions are

$$\sigma_{12} = 0 \qquad (x_1 = x_1\ ,\ x_2 = 0) \tag{5}$$

$$\sigma_{22} = \begin{cases} 0 & (1 < 1x_1\ 1 < \infty\ ,\ x_2 = 0) \\ -p(x_i) & (0 < 1x_1\ 1 < 1\ ,\ x_2 = 0) \end{cases} \tag{6}$$

$$\sigma_{11},\ \sigma_{12},\ \sigma_{22},\ U_1,\ U_2 \to 0\ \ (0 < x_2 < H,\ |x_1| \to \infty) \tag{7}$$

$$\sigma_{11},\ \sigma_{12},\ \sigma_{22},\ U_1,\ U_2 \to 0\ \ ([x_1^2 + x_2^2]^{1/2} \to \infty) \tag{8}$$

and

$$\sigma_{11},\ \sigma_{12},\ \sigma_{22},\ U_1,\ U_2 \text{ continuous } (x_1 = x_1\ ,\ x_2 = H) \tag{9}$$

FORMULATION AND ANALYSIS

It will be useful to recall the definition of the velocities of propagation of dilatational and shear waves, respectively:

$$C_1 = \left[\frac{(\lambda + 2\mu)}{\rho}\right]^{1/2}\ , \qquad C_2 = \left[\frac{\mu}{\rho}\right]^{1/2}. \quad \text{Of course}$$

$$C_1^* = \left[\frac{(\lambda* + 2\mu*)}{\rho*}\right]^{1/2} \qquad C_2^* = \left[\frac{\mu*}{\rho*}\right]^{1/2}.$$

Define the following dimensionless quantities:

$$\xi = \left(\frac{x_1}{H}\right) \qquad \eta = \left(\frac{x_2}{H}\right) \qquad h = \left(\frac{H}{\ell}\right)$$

$$\sigma_{\xi\xi} = \left(\frac{h\sigma_{11}}{\mu}\right) \qquad \sigma_{\eta\eta} = \left(\frac{h\sigma_{22}}{\mu}\right) \qquad \sigma_{\xi\eta} = \left(\frac{h\sigma_{12}}{\mu}\right)$$

$$u = \left(\frac{u_1}{\ell}\right) , \quad v = \left(\frac{u_2}{\ell}\right) \quad , \text{ A Mach number } M = \left(\frac{V}{C_2}\right)$$

$$\alpha = \left(\frac{C_1}{C_2}\right) \qquad \beta = \left(\frac{C_1^*}{C_2}\right) ; \quad \gamma = \left(\frac{C_2^*}{C_2}\right)$$

$$\delta = \left(\frac{\rho^*}{\rho}\right) \quad \text{and} \quad q = \left(-\frac{hp}{\mu}\right)$$

Taking the Fourier transform

$$F\{ \} = (2\pi)^{-1/2} \int_{-\infty}^{\infty} \{ \} \exp (is\,\xi)\, d\xi \tag{19}$$

using further changes in variables and solving simultaneous equations yields for $\rho > 0$;

$$\bar{u} = \left(\beta^2 - M^2\right)^{-1} \left(\beta^2 - \gamma^2\right)^{-1} \left\{ \gamma^2 \beta^2 \bar{v}''' + \left[\left(\beta^2 - \gamma^2\right)^2 - \gamma^2 \left(\gamma^2 - M^2\right)\right]\bar{v}' \right\} \tag{34}$$

and

$$\bar{v}'''' - \left\{ \left[1 - \frac{M^2}{\gamma^2}\right] + \left[1 - \frac{M^2}{\beta^2}\right] \right\} \bar{v}'' + \left[1 - \frac{M^2}{\gamma^2}\right]\left[1 - \frac{M^2}{\beta^2}\right] \bar{v} = 0 \tag{35}$$

Equation 35 has a characteristic equation

$$m^4 - \left\{ \left[1 - \frac{M^2}{\gamma^2}\right] + \left[1 - \frac{M^2}{\beta^2}\right] \right\} m^2 + \left[1 - \frac{M^2}{\gamma^2}\right]\left[1 - \frac{M^2}{\beta^2}\right] = 0 \tag{36}$$

in which s is the characteristic value of $\bar{v} = e^{\alpha}\zeta$. Three cases are possible:

1. Subsonic Case $\quad M^2/\gamma^2 < 1, \ M^2/\beta^2 < 1.$

Letting j, k = $\left[1 - \dfrac{M^2}{\beta^2}\right]^{1/2}, \ \left[1 - \dfrac{M^2}{\gamma^2}\right]^{1/2},$

Equation 36 yields

$$\bar{v} = a^* \cosh j\zeta + b^* \sinh j\zeta + c^* \cosh k\zeta + d^* \sinh k \quad\quad (37)$$

2. Transonic Case $\quad M^2/\gamma^2 > 1, \ M^2/\beta^2 < 1.$

Letting j, k = $\left[1 - \dfrac{M^2}{\beta^2}\right]^{1/2}, \ \left[\dfrac{M^2}{\gamma^2} - 1\right]^{1/2},$

Equation 36 yields

$$\bar{v} = a^* \cosh j\zeta + b^* \sinh j\zeta + c^* \cos k\zeta + d^* \sin k\zeta \quad\quad (38)$$

3. Supersonic Case $\quad M^2/\gamma^2 > 1, \ M^2/\beta^2 > 1.$

Letting j, k = $\left[\dfrac{M^2}{\beta^2} - 1\right], \ \left[\dfrac{M^2}{\gamma^2} - 1\right]^{1/2}$

Equation 36 yields

$$\bar{v} = a^* \cos j\zeta + b^* \sin j\zeta + c^* \cos k\zeta + d^* \sin k\zeta$$

For s < 0, V in both layer and base material takes same form as in Equations 30, 37, 38, and 39 with n replacing s, where n ≡ - s.

SOLUTION OF SHEAR STRESS AT THE INTERFACE
OF THE LAYER AND THE BASE MATERIAL

A. Subsonic Case in Layer and Subsonic Case in Base Material

   1. Solution in Transformed State for s > 0

      Using Equation 37 in Equation 34

$$\bar{u} = a^* k j^{-1} \sinh j\zeta + b^* j^{-1} \cosh j\zeta + c^* k \sinh k\zeta + d^* k \cosh k\zeta \quad\quad (40)$$

and solving gives

$$\tilde{\sigma}_{\xi\eta} (s, 1) = [\tilde{q}_2 (s) - i\tilde{q}_1 (s)] F_1 (s, 1) \qquad (53)$$

2. Solution in Transformed State for $s < 0$

For $s < 0$, V in both layer and base material takes the same form as in Equation 30 and 37 with n replacing s. Carrying out an analysis similar to the case for $s \geq 0$, $\sigma_{\epsilon\eta}$ (n, 1) takes the form

$$\tilde{\sigma}_{\xi\eta} (n, 1) = [\tilde{q}_2 (n) + i\tilde{q}_1 (n)] F_1 (n, 1) \qquad (54)$$

For $s < 0$, with $n \equiv - s$, F_1 (n, 1) takes the same form as F_1 (s, 1) with n replacing s.

Inversion of the solution yields:

$$\sigma_{\xi\eta} (\xi, 1) = (\pi)^{-1} \left\{ \int_0^\infty \int_{-1/h}^{1/h} q (\xi^1) F_1 (s, 1) \right.$$
$$\left. \cdot [\sin s\xi' \cos s\xi - \cos s\xi' \sin s\xi] \, d\xi'ds \right\} \qquad (59)$$

Equation 59 is the general solution at the interface in the form of the double integral for any arbitrary load.

Adding Equations 56 and 58 for the special case of q (ξ) = q_0 ($-1/h \leq \xi \leq 1/h$),

$$\frac{\pi \sigma_{12} (\xi, 1)}{P_0} = 2 \int_0^\infty \frac{F_1 (s, 1)}{s} \sin (s/h) \sin (\xi s) \, ds \qquad (60)$$

Equation 60 is a solution at the interface for a moving uniform load.

DISCUSSION AND CONCLUSION

For Equation 60, σ_{12} (ξ, 1) is seen to be an odd function with respect to ξ because of the term $\sin (p\xi)$ appearing in the integrand of the integral solution σ_{12} (ξ, 1).

By far the most important result is the following. For subsonic speeds (local reference) a material point experiences one stress reversal in shear at the interface over the length of the load. For the transonic case (local reference), a material point experiences several stress reversals in shear at the interface over the length of the load. This phenomenon itself may explain why the bonded layer may fail more easily in the transonic regime than in the subsonic regime by fatigue. Another contributing factor for easier failure in the transonic regime than in the subsonic regime is of course the higher magnitude of the stresses. Experimental evidences (Equations 6, 7, and 8) show such mechanisms for failure.

APPENDIX II
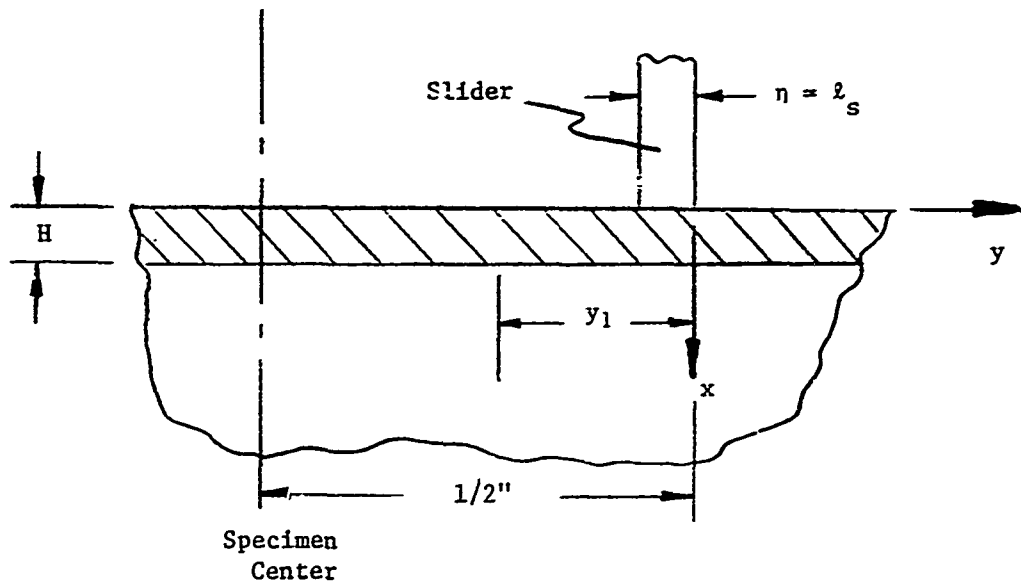
The Boussinesq solution for a punch problem (normal load $P = \pi$)

is:

$$\tau_{xy} = 2 \int_a^b \frac{x^2 y}{[x^2 + y^2]^2} \, dy = \left[\frac{x^2}{x^2 + y^2} \right]_a^b .$$

The Cerruti solution for a punch problem (shear load $S = 0.1\ P$)

is:

$$\tau_{xy} = 0.1 \int_a^b \frac{2xy^2}{[x^2 + y^2]} \, dy = \left[\frac{0.1\ xy}{x^2 + y^2} - 0.1 \arctan \frac{y}{x} \right]_a^b$$

Letting $y = -(y_1 - \eta)$ where $y_1 = 1/4$ inch and evaluate from $\eta = \ell_s$ to

$\eta = 0$, the total shear stress (τ_T) is:

$$\tau = \left[\frac{x^2}{x^2 + y^2} - \frac{1}{2} + \frac{0.1xy}{x^2 + y^2} - 0.1 \arctan \frac{y}{x} \right]_{-\ell_s}^{0}$$

(the subscript has been dropped and $y \equiv y_1$)

For: $x = H = 0.001$ inch

$\qquad y = y_1 = 0.250$ inches

$\qquad \ell_s = 0.025$ inches

$\qquad \tau \cong = 0.000027$

$\qquad\qquad$ Maximum shear stress occurs at $x = H$, $y = \ell_s$.

For: $x = H = 0.001$ inch

$\qquad y = y_1 = \ell_s = 0.025$ inches

$\qquad \tau_{max} = 1.137$

$\dfrac{\tau}{\tau_{max}}$ x 100 $\approx$ 0.0023% or approximately no stress reversal when

slider is at end of stroke.